

Handbook of
Selected Tissue Doses
for
Fluoroscopic and Cineangiographic
Examination of the Coronary Arteries

Stanley H. Stern, Ph.D. and Marvin Rosenstein, Ph.D.
Center for Devices and Radiological Health
Food and Drug Administration

•
Louis Renaud, PEng., Ph.D.
Service de Génie Biomédical
Institut de Cardiologie de Montréal

•
Maria Zankl, Ph.D.
Institut für Strahlenschutz
GSF – Forschungszentrum für Umwelt und Gesundheit GmbH



September 1995

U.S. DEPARTMENT OF HEALTH AND HUMAN SERVICES
Public Health Service
Food and Drug Administration
Center for Devices and Radiological Health
Rockville, Maryland 20850

DESCRIPTION OF THE HANDBOOK

Introduction

This Handbook contains data from which absorbed dose in selected tissues can be estimated for fluoroscopic and cineangiographic examinations of the coronary arteries of adults represented by a reference male and a reference female anthropomorphic phantom (Appendix A). The Handbook is designed to permit users to evaluate tissue doses in reference adults for the range of examination conditions prevalent in clinical facilities. Since the variation in anthropometric characteristics of real people is not considered, assignment of the data to individual patients may lead to misestimation of tissue doses, except for absorbed dose in the entrance skin in the primary field.

Handbook Tables 1 through 11 are each based on a distinct x-ray field commonly used in coronary interventional radiology. Associated with each field are a view, an arterial projection, and technique factors such as tube potential (kVp), half-value layer (HVL), source-to-skin distance (SSD), source-to-image-receptor distance (SID), and field-of-view (FOV) diameter at the image receptor, where all fields of view were modeled as circular. The selection of the x-ray fields derives from analyses of practice primarily at the Institut de Cardiologie de Montréal (1), particularly from a study (2) of 230 examinations conducted in 1988. Although the set of x-ray fields corresponds to the experience at one clinic, the scope of views and arterial projections represented make the Tables generally applicable to approximate a broad range of examinations following a variety of clinical protocols in many different venues.

Table entries are presented as conversion coefficients (CC), i.e., as absorbed dose in a specific tissue per unit x-ray exposure determined free-in-air (and without the presence of a supporting tabletop) at a reference plane corresponding to where the skin-entrance plane would be. The Handbook user must supply estimates of the entrance skin exposures associated with the examination to estimate absorbed doses.

For each tissue, conversion coefficients are calculated from a Monte Carlo computer code simulating radiation transport in mathematical, anthropomorphic gender-differentiated phantoms. These phantoms and codes have evolved for calculations in medical dosimetry over a number of years (3-6). The ADAM (male) and EVA (female) versions used for this Handbook were developed at the Institut für Strahlenschutz, GSF — Forschungszentrum für Umwelt und Gesundheit (5,6). ADAM is a modification of the original MIRD-5 phantom of the Medical Internal Radiation Dose Committee (3). EVA is the ADAM phantom reduced uniformly to 83 percent of its original size, with the testes excluded and the ovaries, uterus, and female breasts included (5). An esophagus has recently been incorporated in both

phantoms (6), and for this Handbook the conversion coefficient for the colon is the mass-weighted sum of conversion coefficients for the upper large intestine and lower large intestine. The simulations have no modeling, however, to incorporate contrast media used in examinations of the coronary arteries.

In order to model the variable attenuation of x rays through an intervening tabletop for all views, a supporting tabletop composed of tissue-equivalent material was added to the computer code. The supporting tabletop is 250 cm long, 60 cm wide and 0.7 cm thick. The phantoms were centered with the back on top of the supporting tabletop. There was no modeling of tabletop padding used for patient comfort; such padding would tend to harden the x-ray field incident on a patient.

Acronyms and special terminology used in the Handbook generally are defined when they are introduced and are also compiled in a Glossary on pages xiv and xv.

Index of Handbook Tables

Conversion Coefficients for Fluoroscopy and Cineangiography of the Coronary Arteries

Table Number	View ^a	Page Number
1	RAO 30° (left)	1
2	RAO 30° (right)	2
3	LAO 30° (right)	3
4	LLAT (left)	4
5	RAO 15° Caudal 25° (left)	5
6	RAO 15° Cranial 25° (left)	6
7	Cranial 20° (right)	7
8	LAO 45° Cranial 25° (left)	8
9	LAO 45° (left)	9
10	RAO 10° Cranial 40° (left)	10
11	Anterior (left)	11
12	Nominal Conversion Coefficients	12

^a"Left" or "right" in parentheses refers to the left or right ventricle whose center is the "field center" toward which the central ray is directed in a particular view.

View-by-View Analysis of an Examination (Tables 1 through 11)

Tables 1 through 11 are used with the instructions for Method A, which describe a view-by-view analysis of an examination. These Tables are titled by the views they represent — right anterior oblique (RAO), left anterior oblique (LAO), left lateral (LLAT), cranial, and caudal. Labeling of the views conforms to the conventions of interventional cardiac radiology, where views are designated from the perspective of the image-receptor looking at the patient. The field center is the left ventricle for Tables 1, 4-6, 8-11; the field center is the right ventricle for Tables 2, 3 and 7. Figure B-1 in Appendix B illustrates the irradiation geometry and labeling conventions. Table B-1 provides the phantom coordinates that locate the left and right ventricle centers. Figure B-2 depicts the intersections of the x-ray fields and skin-entrance planes. The specific arteries visualized in each view are indicated in the information above each Table, and arterial locations about the heart are depicted in Appendix C, Figure C-1.

Associated with each entry of Tables 1 through 11 is a measure of the statistical uncertainty of a conversion coefficient derived from the simulations by the Monte Carlo technique. The statistical uncertainty referred to is the standard deviation (SD) of the mean value (4,7) of the conversion coefficient for a particular phantom gender, irradiation geometry, tissue and HVL. The mean value is the conversion coefficient resulting from Monte Carlo simulations of radiation transport initiated with 5 million incident photons, and it is the entry value presented in the Tables. The coefficient of variation (CV) is the ratio of the standard deviation of the mean to the magnitude of the mean:

$$\text{CV (in percent)} = \frac{100 \times \text{one } SD_{\text{mean}}}{\text{conversion coefficient}} .$$

Each row of entries in Tables 1 through 11 represents a group of conversion coefficients for a specified tissue. For each row, the entry in the column labeled "Max. CV" is the maximum value (in percent) among the CV's associated with the conversion coefficients for that tissue.

Nominal Analysis of an Examination (Table 12)

The entries of Table 12 are provided as "Nominal Conversion Coefficients." A nominal conversion coefficient is defined as the arithmetic mean of the corresponding entries of Tables 1 through 11, each value averaged respective to tissue and HVL. Table 12 is used with the instructions for Method B, in which an examination is characterized in an overall sense. Use of Table 12 with Method B offers a quick, but less accurate, way to estimate nominal tissue doses for a complete examination without detailed specifications for the particular views applied

clinically. This approach is acceptable for coronary artery examinations because all of the views share the heart as a relatively small, common, central region intercepted by the central ray of each different x-ray field. The approach, however, would not be valid, for example, for upper gastrointestinal fluoroscopic examinations, where there is no single common locus of the multiple x-ray fields.

Associated with each entry of Table 12 is a measure of the spread of the related values presented in Tables 1 through 11, namely, the standard deviation (SD) of the distribution of related conversion coefficients. In Table 12, the coefficient of variation (labeled " CV_{nom} ") is the ratio of the standard deviation to the nominal conversion coefficient:

$$CV_{nom} \text{ (in percent)} = \frac{100 \times \text{one SD}}{\text{nominal conversion coefficient}}$$

In Table 12, the entry in the column labeled "Max. CV_{nom} " is the maximum value (in percent) among the CV_{nom} 's associated with the nominal conversion coefficients for that tissue. For any particular tissue, one expects a discrepancy from using Table 12 instead of any other single Table. The magnitude of the maximum discrepancy (in percent) is the Max. CV_{nom} . Because clinical examinations typically involve multiple views, the differences between results evaluated from Table 12 and those evaluated from the other relevant Tables will usually be smaller than the Max. CV_{nom} values in Table 12.

Radiation Quantities and Units

Conversion coefficients are presented in units of *mrad* (absorbed dose in tissue) *per 1 R* (entrance skin exposure), where the entrance skin exposure is determined free-in-air at a reference plane corresponding to the skin-entrance plane. To express these conversion coefficients in units of the Système International (SI), divide the Table entries by **25.8** to obtain values as *mGy* (absorbed dose in tissue) *per 1-mC/kg* (entrance skin exposure) (8), or divide the entries by **0.876** to obtain values as *mGy* (absorbed dose in tissue) *per 1 Gy* (air kerma) (9).

Beam Quality

Conversion coefficients are provided for six beam qualities, three for the male (2.5, 4.0 and 5.5 mm Al HVL) and three for the female (2.0, 3.5 and 5.0 mm Al HVL). The range of each HVL set corresponds to a spread of ± 2 standard deviations about respective mean tube potentials observed in the study (2) conducted at the Institut de Cardiologie de Montréal. HVL measurements are free-in-air and without the presence of a supporting tabletop. The overall range of HVL covered in the

Handbook corresponds to that observed in a nationwide survey of fluoroscopy practice in the United States (10).

In practice, beam quality is associated with a variety of different combinations of tube potential, filtration (i.e., exclusive of tabletop), and waveform. For the Monte Carlo calculations of conversion coefficients, six representative x-ray spectra were generated at GSF to match the range of tube potentials and HVLs observed in the Institut de Cardiologie de Montréal study (2). The beam qualities for the six x-ray spectra are:

Male			Female		
Peak Tube Potential (kV)	Total Filtration (mm Al)	HVL (mm Al)	Peak Tube Potential (kV)	Total Filtration (mm Al)	HVL (mm Al)
60	3.5	2.5	50	3.3	2.0
90	4.0	4.0	80	3.9	3.5
120	4.3	5.5	110	4.2	5.0

For the usual ranges of these parameters in fluoroscopy and cineangiography of the coronary arteries, one can approximate the beam quality with a single parameter, namely, HVL, irrespective of values of the other associated parameters. This approximation is adopted in this Handbook. For these examinations, the approximation contributes an uncertainty of less than about ± 10 percent in the value of the conversion coefficients when actual tube potentials and total filtrations differ from those listed for the HVLs above.

Irradiation Geometry

In the radiation transport simulations, reference values of SSD, SID, FOV_{Table} diameter at the image-receptor (IR) plane, and view angles were used, as cited in each Table. In actual clinical examinations, the values of these parameters may differ from the reference values. Variations in SSD, SID, and FOV at the IR plane were evaluated with an independent computer program (11) yielding the following results:

(1) **FOV fixed**

For anterior and lateral views with a field-of-view area fixed at 113 cm², conversion coefficients were evaluated for lung, active bone marrow, thyroid, and trunk tissue. For each tissue at each of two beam qualities (2.0- and 5.5-mm Al HVL), the conversion coefficients varied by approximately $\pm 20\%$ over the ranges of SSD (50 to 70 cm) and SID (80 to 110 cm) evaluated.

- (2) **SSD and SID fixed**
 With these same beam qualities and views, for a fixed SSD (60 cm) and fixed SID (90 cm), respective conversion coefficients were found to be approximately proportional to the FOV area (i.e., over the range 95 to 415 cm²) at the IR plane.
- (3) **FOV, SSD, and SID varied**
 Within an HVL range of 3.0 to 5.1 mm Al and with an anterior view, an ensemble of values of SSD (46 to 73 cm), SID (92 to 113 cm), and FOV area (181 to 412 cm²) were varied independently of each other. For a specific beam quality and tissue, irrespective of SSD and SID, ratios of conversion coefficients were approximated by corresponding ratios of FOV areas to within a relative uncertainty of about $\pm 40\%$, that is:

$$CC_{\text{area } 1} / CC_{\text{area } 2} \approx \text{FOV area}_1 / \text{FOV area}_2.$$

On the basis of these results, when the clinical FOV diameter differs from the reference FOV_{Table} diameter by more than $\pm 20\%$, irrespective of how much the clinical SSD and SID may differ from the reference SSD and SID listed in a Table, it is recommended that an FOV correction be applied to tabulated conversion coefficients. (See Instructions on pages xi and xii.)

Tissues

The tissues selected for presentation in the Handbook fall into three categories:

(1) **Entrance Skin in the Primary Field**

The tissue at greatest risk for deterministic injury is that portion of skin lying directly in the path of the incident primary field. In the Tables, this portion is designated "entrance skin in primary field," (abbreviated "ESPF"), and its conversion coefficients are highlighted in a shaded row. The entrance skin in the primary field is only a small fraction of the entire skin tissue; the extent is delimited and the location is determined by the collimation and irradiation geometry modeled in the simulations. For each of the views in the Handbook, the entrance skin in the primary field surrounds the skin-entry point of the central ray of the x-ray beam and occupies an approximately elliptical area on the plane tangent to the phantom surface at this point; the thickness of the skin modeled in the computer code is 0.2 cm. The location of each region of ESPF is different for each view. Figure B-2 in Appendix B displays the locus of the entrance-skin area for each of the anterior/oblique views modeled in the Handbook. For an examination that entails use of multiple views, this figure can serve as a guide to indicate the extent of primary-field overlap in a subportion of entrance-skin.

(2) **Internal Tissues with Associated Stochastic Health Effects**

Tissues for which the International Commission on Radiological Protection (ICRP) (12) has provided risk coefficients for cancer mortality, genetic effects, and *in utero* effects are the brain, thyroid, thymus, active bone marrow, esophagus, lung, adrenal, spleen, pancreas, stomach, liver, kidney, colon, small intestine, urinary bladder, and breast, ovary, and uterus for the female, and testis for the male.

The average absorbed dose in the uterus is used to approximate the absorbed dose in the embryo. This approximation is strictly applicable only in the first two months of pregnancy.

(3) **The Heart**

The heart surrounds the ventricle isocenters and always lies within the field of view. Of all internal organs, it typically receives the highest absorbed dose per unit entrance skin exposure and the highest cumulative absorbed dose for a complete examination. Conversion coefficients for the heart are provided for reference only; there is no health effect yet established for absorbed doses in the ranges that occur in these examinations.

Except for the conversion coefficients cited for the entrance skin in the primary field, each other entry corresponds to the absorbed dose averaged over the entire mass of specified tissue, e.g., right and left lungs, right and left ovaries, all of the active bone marrow distributed throughout the body.

INSTRUCTIONS FOR USE OF HANDBOOK

The following instructions offer two ways of computing absorbed doses in tissues from fluoroscopic and cineangiographic examinations of the coronary arteries.

Method A: The instructions provide a more accurate, but information-intensive method in which all of the views used clinically are analyzed in detail. **Method B:** The instructions provide a less accurate method in which general observations are used to represent the examination with nominal values of the important factors that affect the magnitude of absorbed doses. Method B is recommended for routine assessments.

Method A: View-by-View Analysis of an Examination (Tables 1 through 11) – A sample calculation is provided in Appendix D.

1. Represent examination views

Appendix D, Table D-1, gives a sample data array for an actual sequence of examination segments and their association with Handbook Tables 1 through 11.

- a. For each view being represented, select the Table whose angulations are closest to those of the clinical view. First consider transverse angulation. Second consider sagittal angulation.
- b. Disregard differences between the SSD and SID given in a Table and those values actually used in the examination.

2. Determine entrance skin exposures

To estimate tissue doses, it is essential that a user know the radiation output of the x-ray systems for the modes applied in the examination. Following Instruction 1, group the examination segments according to common view and the applicable Table. For each group, determine the skin-entrance exposure (free-in-air). Exposure values are needed for the fluoroscopic and the cineangiographic components. Fluoroscopic exposure may be evaluated as the product of fluoroscopic exposure rate and fluoroscopic exposure time. Cineangiographic exposure may be evaluated as the product of the cineangiographic exposure rate (per frame rate) and the number of cine frames.

Appendix D, Table D-2, gives an example of how exposures are determined for each group of examination segments associated with a common view and applicable Table.

3. **Determine applicable HVLs and Field of View corrections**

For each group of examination segments associated with a Table,

a) ***Select HVL.***

For each group, enter the Table at the HVL closest to the estimate of the actual clinical HVL: 2.5, 4.0, or 5.5 mm Al for males; 2.0, 3.5, or 5.0 mm Al for females.

b) ***Correct for Field of View (FOV).***

If the actual clinical FOV diameter at the image-receptor plane for a group differs by more than $\pm 20\%$ from the reference Monte Carlo FOV diameter in the Table, calculate the correction factor as follows:

$$(\text{FOV}_{\text{group}}/\text{FOV}_{\text{Table}})^2.$$

This correction factor is applicable for all tissues doses except the entrance skin in the primary field (ESPF). No FOV correction is to be applied for ESPF.

Note:

$\text{FOV}_{\text{group}}$ is the average field-of-view diameter for a group of clinical examination segments.

$\text{FOV}_{\text{Table}}$ is the field-of-view diameter specified in each Table for the Monte Carlo simulation.

Appendix D, Table D-3, gives the HVL selections and FOV corrections for the sample examination represented in Tables D-1 and D-2.

4. **Select conversion coefficients**

For each group of examination segments associated with a Table (1 through 11), select conversion coefficients according to the HVLs from Instruction 3. See Appendix D, Table D-4.

5. **Compute tissue doses for each view**

For each group of examination segments associated with a Table (1 through 11), multiply the conversion coefficients from Instruction 4 by the corresponding entrance skin exposures determined in Instruction 2. For all tissues except the entrance skin in the primary field (ESPF), the tissue dose is this product times the FOV correction factor determined in Instruction 3. For ESPF, the dose is simply the product without any FOV correction factor. See Appendix D, Table D-4.

6. **Compute tissue doses for examination**

The cumulative tissue doses for the examination are the sums of the contributions from each view in Instruction 5. See Appendix D, Table D-4.

Method B: Nominal Analysis of an Examination (Table 12) – A sample calculation is provided in Appendix E.

1. Characterize the complete examination, irrespective of view and fluoroscopic or cineangiographic mode, with a single nominal value for each of the following four parameters:
 - (a) HVL,
 - (b) total entrance skin exposure (free-in-air) for all the fluoroscopic plus cineangiographic segments (i.e., summed for all skin-entrance planes, wherever these planes are located),
 - (c) FOV_{nominal} diameter at the image-receptor plane, and
 - (d) the highest cumulative entrance exposure (i.e., fluoroscopic plus cineangiographic) at any single skin location. Such a skin region may be irradiated in only one view or possibly in multiple views that share a common locus of irradiation.
2. Using the nominal HVL from Instruction 1.a, select the conversion coefficients in Table 12 for each tissue of interest. Linear interpolation between HVLs is recommended when the nominal HVL is different than the tabulated HVLs.
3. If the FOV_{nominal} diameter from Instruction 1.c is more than $\pm 20\%$ different than 14 cm, the FOV correction factor for all tissues except the entrance skin in the primary field (ESPF) is computed as follows:

$$(\text{FOV}_{\text{nominal}}/14 \text{ cm})^2.$$

No FOV correction is to be applied for the entrance skin in the primary field.

Note:

FOV_{nominal} is a single value for the complete clinical examination, taken as an average field-of-view diameter for all segments (irrespective of view and fluoroscopic or cineangiographic mode).

The value of 14 cm (from Table 12) is the average of the FOV diameters given in Tables 1-11.

4. For each tissue except the entrance skin in the primary field, the absorbed dose is the product of the interpolated conversion coefficient (Instruction 2), the total entrance skin exposure for all examination segments (Instruction 1b), and the FOV correction factor (Instruction 3, if applicable).
5. The maximum absorbed dose in the entrance skin *at any single location* in the primary field(s) is the product of the interpolated conversion coefficient (Instruction 2) and the highest cumulative entrance skin exposure (Instruction 1d) at any single skin location.

Appendix E, Table E-1, illustrates how Method B is applied to the sample examination. In that sample, the nominal values for the four parameters (Instruction 1a-1d) were

determined from the measured data detailed in Tables D-1 through D-3. In practice, most users will not have access to such detailed data, and they will have to rely on their best overall estimates of nominal values for the four parameters.

A comparison of results of Methods A and B is given in Appendix F; and a synopsis of results for the sample examination is given in Appendix G.

Glossary

ABM	active bone marrow
applicable Handbook Table	Table whose view most closely represents the view of a group of segments of a clinical examination, selected according to Instructions for Method A
applicable HVL	half-value layer entry to a Table: most closely represents the HVL of a group of segments of a clinical examination, selected according to Instructions for Method A
CA	coronary angiography
caud	caudal
CC	conversion coefficient
cine	cineangiographic
conversion coefficient	absorbed dose in a specific tissue per unit x-ray exposure (free-in-air at the skin-entrance plane), tabulated in Tables 1-11
cran	cranial
CV	coefficient of variation: the ratio of the standard deviation of the mean to the magnitude of the mean, where "mean" refers to any of the conversion coefficient values cited in Tables 1-11
CV_{nom}	coefficient of variation for nominal (Table 12) conversion coefficient: ratio of standard deviation of the distribution (Tables 1-11) of conversion coefficients to nominal conversion coefficient (Table 12)
diam	diameter
ESPF	entrance skin in primary field
fluoro	fluoroscopic
FOV	field of view at the image-receptor plane
FOV_{group}	average field-of-view diameter (at image-receptor plane) for a group of fluoroscopic or cineangiographic clinical examination segments that share a common view, grouped according to Instructions for Method A
FOV_{nominal}	nominal field-of-view diameter (at image-receptor plane): a single value for the complete clinical examination, taken as an average field-of-view diameter for all segments (irrespective of view and fluoroscopic or cineangiographic mode), applied according to Instructions for Method B

Glossary (continued)

FOV_{Table}	field-of-view diameter (at image-receptor plane) specified in each Table, used to define the size of the x-ray field in the Monte Carlo simulation generating the conversion coefficients
group of examination segments	a set of clinical fluoroscopic or cineangiographic examination segments sharing a common view and associated with a specific Table, used in Method A
HVL	half-value layer
image-receptor plane	x-ray entrance plane at the input screen of the image-intensifier tube
IR	image receptor
kVp	peak x-ray tube potential
LAO	left anterior oblique
LCA	left coronary angiography
LLAT	left lateral
LV	left ventriculogram
Max. CV	maximum value among the coefficients of variation associated with the conversion coefficients for a particular tissue (see Tables 1-11)
Max. CV_{nom}	maximum value among the coefficients of variation associated with the nominal conversion coefficients for a particular tissue (see Table 12)
nominal conversion coefficient	conversion coefficient tabulated in Table 12 as the mean value of the corresponding entries of Tables 1-11, applied according to Instructions for Method B
nominal HVL	a single value for the complete clinical examination, taken as an average half-value layer for all segments (irrespective of view and fluoroscopic or cineangiographic mode), applied according to Instructions for Method B
RAO	right anterior oblique
RCA	right coronary angiography
SD	standard deviation
SD_{mean}	standard deviation of the mean
SID	source-to-image-receptor distance
SSD	source-to-skin distance

Acknowledgments

The authors thank Dr. Madeline V. Pina of Fairfax Hospital, Falls Church, Virginia, for facilitating observations of examinations at the cardiac catheterization laboratories there and for comments on the manuscript. They also thank Drs. Michael J. Dennis and David L. Hykes, Sr., for making available results of related work at the Medical College of Ohio. The authors gratefully acknowledge the review of Dr. Thomas B. Shope, Jr., of the Center for Devices and Radiological Health.

REFERENCES

1. Lespérance, J. *Coronary Angiography — Projections*. Radiology Department Report. Institut de Cardiologie de Montréal (April 1982).
2. Haddadi, Rached et Louis Renaud. *Projections et Conditions Techniques en Usage en Angiocardiologie. Étude Statistique*. Rapport Technique, Service de Génie Biomédical, Institut de Cardiologie de Montréal (March 1993).
3. Snyder, W.S., M.R. Ford, G.G. Warner, and W.L. Fisher, Jr. *Estimates of Absorbed Fractions for Monoenergetic Photon Sources Uniformly Distributed in Various Organs of a Heterogeneous Phantom*. Journal of Nuclear Medicine, Supplement Number 3, Pamphlet 5 (August 1969).
4. Rosenstein, M. *Organ Doses in Diagnostic Radiology*. HEW Publication (FDA) 76-8030, U.S. Food and Drug Administration, Rockville, Maryland (1976).
5. Kramer, R., M. Zankl, G. Williams, and G. Drexler. *The Calculation of Dose from External Photon Exposures Using Reference Human Phantoms and Monte Carlo Methods. Part I: The Male (ADAM) and Female (EVA) Adult Mathematical Phantoms*. GSF-Bericht S-885. Gesellschaft für Strahlen- und Umweltforschung mbH, München (December 1982, reprinted January 1986).
6. Zankl, M., N. Petoussi, and G. Drexler. *Effective Dose and Effective Dose Equivalent — The Impact of the New ICRP Definition for External Photon Irradiation*. Health Physics, Volume 62, Number 5, pp. 395-399 (May 1992).
7. Carter, L.L., and E.D. Cashwell. *Particle-Transport Simulation with the Monte Carlo Method*. U.S. Energy Research and Development Administration, Technical Information Center, Office of Public Affairs, TID-26607, Oak Ridge, Tennessee, (October 1975).

8. *Radiation Quantities and Units*. ICRU Report 33. International Commission on Radiation Units and Measurements, Bethesda, Maryland (April 1980).
9. *Measurement of Dose Equivalents from External Photon and Electron Radiations*. ICRU Report 47. International Commission on Radiation Units and Measurements, Bethesda, Maryland (April 1992).
10. Conway, Burton J., in association with the CRCPD Committee (H-4) on Nationwide Evaluation of X-Ray Trends. *Nationwide Evaluation of X-Ray Trends (NEXT) Summary of 1990 Computerized Tomography Survey and 1991 Fluoroscopy Survey*. CRCPD Publication 94-2. Conference of Radiation Control Program Directors, Frankfort, Kentucky (January 1994).
11. Peterson, Leif E., and Marvin Rosenstein. *Computer Program for Tissue Doses in Diagnostic Radiology (for VAX and IBM-Compatible PC Systems)*. U.S. Food and Drug Administration, Center for Devices and Radiological Health, Rockville, Maryland (1989).
12. *1990 Recommendations of the International Commission on Radiological Protection*. ICRP Publication 60. Annals of the ICRP, Volume 21, No. 1-3. Pergamon Press, Oxford (1991).
13. "The National Heart, Lung, and Blood Institute Coronary Artery Surgery Study (CASS)." *Circulation*, Volume 63, supplement I, (June 1981).
14. "Protocol for the Bypass Angioplasty Revascularization Investigation (BARI)," *Circulation*, Volume 84, supplement V, (December 1991); *BARI-CRL Operations Manual*, Appendix A. Supplemental Definitions, Stanford University Medical Center, Palo Alto, California, (May 1989).
15. Hykes, David Lewis, Sr. *Determination of Patient Radiation Doses Associated with Cardiac Catheterization Procedures using Direct Measurements and Monte Carlo Methods*. Ph.D. dissertation. Medical College of Ohio, Toledo, Ohio, pp. 80-81, (1994).
16. Wagner, L.K., P.J. Eifel, and R.A. Geise. "Potential Biological Effects Following High X-ray Dose Interventional Procedures." *Journal of Vascular and Interventional Radiology*, Volume 5, pp. 71-84 (1994).

Table 1. RAO 30° (left)
tissue dose (mrad) per 1-R exposure (free-in-air at skin-entrance plane)^a

Angulation^b of image receptor: transverse -30°, sagittal 0°. Field center^b: left ventricle.
SSD = 60 cm; SID = 90 cm; FOV_{Table} diameter at image receptor = 14 cm.

Arteries^c visualized: LM; mid, dis Cx; M₂, M₃; prox, dis LAD; D₁; *ld*: LAV, LPLS, Crux, LPDA

HVL (mm Al)	2.5	4.0	5.5	2.0	3.5	5.0	Max. CV (%) ^d
Tissue	Male			Female			
Entrance skin in primary field	880	981	1033	831	957	1021	0.2
Brain	0.004	0.023	0.050	0.001	0.022	0.049	12.6
Thyroid	0.15	0.64	1.0	0.10	0.61	1.2	9.5
Thymus	3.0	8.3	11.8	2.1	8.4	14.3	2.2
Active bone marrow	4.6	8.3	11.0	4.2	8.7	12.6	0.1
Esophagus	20.3	41.0	55.5	17.2	42.5	63.3	0.7
Lung	55.7	81.7	96.6	50.6	83.9	104	0.1
Breast				3.0	10.1	16.1	0.5
Heart	48.1	93.5	125	38.1	92.9	134	0.2
Adrenal	8.2	17.2	22.9	6.4	17.5	25.7	1.5
Spleen	7.0	14.8	19.6	5.4	14.7	21.5	0.6
Pancreas	6.1	14.6	20.3	4.3	14.2	22.2	0.8
Stomach	3.8	9.0	12.5	2.7	8.7	13.5	0.8
Liver	1.6	4.5	6.9	1.1	4.5	7.7	0.5
Kidney	1.0	2.8	4.3	0.70	2.8	4.8	1.2
Colon	0.057	0.26	0.45	0.033	0.26	0.54	3.9
Small intestine	0.069	0.33	0.58	0.038	0.31	0.66	2.7
Ovary				0.005	0.069	0.15	54.2
Uterus				0.005	0.069	0.14	24.4
Urinary bladder	0.001	0.017	0.045	0.001	0.018	0.042	42.7
Testis	+	+	0.006				66.8

^aDivide table entries (mrad per R) by 25.8 to get SI units of (mGy per mC/kg exposure), by 0.876 to get (mGy per Gy air kerma).

^bSee Appendix B, Irradiation Geometry.

^cSee Appendix C, Coronary Artery Nomenclature

^dMaximum coefficient of variation in percent.

+ Less than 0.001 mrad per R.

Table 2. RAO 30° (right)
tissue dose (mrad) per 1-R exposure (free-in-air at skin-entrance plane)^a

Angulation^b of image receptor: transverse - 30°, sagittal 0°. Field center^b: right ventricle.
SSD = 60 cm; SID = 90 cm; FOV_{Table} diameter at image receptor = 14 cm.

Arteries^c visualized: mid RCA; rd: RPDA

HVL (mm Al)	2.5	4.0	5.5	2.0	3.5	5.0	Max. CV (%) ^d
Tissue	Male			Female			
Entrance skin in primary field	878	975	1028	831	957	1022	0.2
Brain	0.004	0.025	0.050	0.001	0.023	0.053	13.9
Thyroid	0.18	0.65	1.1	0.087	0.64	1.3	9.1
Thymus	3.0	8.3	12.1	2.1	8.6	14.2	2.2
Active bone marrow	4.4	7.8	10.4	4.0	8.3	11.8	0.1
Esophagus	18.6	36.6	49.4	15.7	39.5	57.1	0.7
Lung	58.7	85.7	101	53.2	88.0	109	0.1
Breast				3.4	11.1	17.6	0.5
Heart	47.9	92.7	124	38.0	91.8	132	0.2
Adrenal	7.6	16.5	22.2	5.8	16.7	24.4	1.6
Spleen	7.4	15.3	20.3	5.7	15.4	22.2	0.6
Pancreas	6.1	14.6	20.6	4.4	14.3	21.8	0.8
Stomach	3.9	9.3	13.0	2.8	9.1	14.2	0.8
Liver	1.6	4.4	6.7	1.1	4.4	7.6	0.5
Kidney	1.0	2.8	4.2	0.70	2.8	4.8	1.2
Colon	0.056	0.26	0.45	0.034	0.26	0.55	3.8
Small intestine	0.070	0.33	0.58	0.036	0.31	0.66	2.7
Ovary				0.006	0.065	0.16	49.4
Uterus				0.006	0.052	0.14	19.8
Urinary bladder	0.001	0.018	0.039	0.002	0.016	0.044	38.4
Testis	0.001	0.002	0.003				100.0

^aDivide table entries (mrad per R) by 25.8 to get SI units of (mGy per mC/kg exposure), by 0.876 to get (mGy per Gy air kerma).

^bSee Appendix B, Irradiation Geometry.

^cSee Appendix C, Coronary Artery Nomenclature

^dMaximum coefficient of variation in percent.

+ Less than 0.001 mrad per R.

Table 3. LAO 30° (right)
tissue dose (mrad) per 1-R exposure (free-in-air at skin-entrance plane)^a

Angulation^b of image receptor: transverse 30°, sagittal 0°. Field center^b: right ventricle.
SSD = 60 cm; SID = 90 cm; FOV_{Table} diameter at image receptor = 12 cm.

Arteries^c visualized: prox, mid, dis RCA; *rd*: RPDA, Crux, RPLS

HVL (mm Al)	2.5	4.0	5.5	2.0	3.5	5.0	Max. CV (%) ^d
Tissue	Male			Female			
Entrance skin in primary field	874	974	1021	829	954	1012	0.2
Brain	0.003	0.015	0.031	0.001	0.014	0.036	12.6
Thyroid	0.11	0.42	0.69	0.058	0.46	0.90	10.3
Thymus	2.1	5.7	8.4	1.4	5.9	9.6	2.3
Active bone marrow	3.4	6.2	8.4	3.0	6.5	9.4	0.1
Esophagus	8.7	20.6	28.6	6.4	20.5	32.3	0.9
Lung	37.9	55.5	65.6	35.2	57.9	71.7	0.1
Breast				1.6	6.1	10.1	0.6
Heart	34.8	69.3	93.5	27.9	69.5	102	0.2
Adrenal	6.2	13.4	17.9	4.6	12.8	19.6	1.5
Spleen	0.32	1.3	2.2	0.18	1.3	2.4	2.5
Pancreas	1.8	5.0	7.8	1.2	5.0	8.7	1.3
Stomach	0.53	1.8	3.0	0.34	1.8	3.4	1.8
Liver	5.3	11.2	15.1	4.1	11.2	16.5	0.2
Kidney	0.75	2.1	3.2	0.49	2.1	3.5	1.2
Colon	0.044	0.19	0.34	0.023	0.19	0.40	4.1
Small intestine	0.050	0.22	0.41	0.024	0.22	0.46	2.8
Ovary				0.002	0.043	0.12	41.4
Uterus				0.003	0.040	0.11	21.2
Urinary bladder	0.001	0.014	0.027	0.001	0.012	0.033	40.5
Testis	+	0.002	0.002				69.5

^aDivide table entries (mrad per R) by 25.8 to get SI units of (mGy per mC/kg exposure), by 0.876 to get (mGy per Gy air kerma).

^bSee Appendix B, Irradiation Geometry.

^cSee Appendix C, Coronary Artery Nomenclature

^dMaximum coefficient of variation in percent.

+ Less than 0.001 mrad per R.

Table 4. LLAT (left)
tissue dose (mrad) per 1-R exposure (free-in-air at skin-entrance plane)^a

Angulation^b of image receptor: transverse 90°, sagittal 0°. Field center^b: left ventricle.
SSD = 50 cm; SID = 90 cm; FOV_{Table} diameter at image receptor = 15 cm.

Arteries^c visualized: mid, dis Cx; M₂, M₃; LAV; mid, dis LAD; D₁; D₂; D₃

HVL (mm Al)	2.5	4.0	5.5	2.0	3.5	5.0	Max. CV (%) ^d
Tissue	Male			Female			
Entrance skin in primary field	946	1006	1040	922	992	1028	0.2
Brain	0.002	0.020	0.037	0.001	0.015	0.041	14.1
Thyroid	0.11	0.43	0.71	0.050	0.47	0.89	12.1
Thymus	1.5	4.6	7.1	1.1	4.7	8.2	2.7
Active bone marrow	1.7	3.6	5.1	1.5	3.9	6.0	0.1
Esophagus	3.3	9.8	15.0	2.6	10.3	17.7	1.5
Lung	17.6	33.3	44.1	15.6	35.6	50.4	0.2
Breast				3.6	9.5	14.1	0.4
Heart	16.6	37.5	53.2	13.6	39.5	61.0	0.3
Adrenal	1.4	4.1	6.9	0.88	4.3	7.8	3.5
Spleen	0.24	1.1	1.8	0.14	1.0	2.1	3.2
Pancreas	0.87	3.2	5.1	0.56	3.2	5.8	2.0
Stomach	0.39	1.5	2.5	0.25	1.5	2.9	2.3
Liver	3.9	9.6	13.8	2.9	9.9	15.6	0.3
Kidney	0.27	1.0	1.8	0.16	1.0	2.1	2.1
Colon	0.031	0.15	0.28	0.017	0.16	0.36	4.9
Small intestine	0.034	0.18	0.35	0.017	0.18	0.41	3.6
Ovary				0.002	0.040	0.070	47.7
Uterus				0.001	0.034	0.088	31.6
Urinary bladder	0.001	0.009	0.019	+	0.010	0.033	61.0
Testis	+	0.001	0.001				73.6

^aDivide table entries (mrad per R) by 25.8 to get SI units of (mGy per mC/kg exposure), by 0.876 to get (mGy per Gy air kerma).

^bSee Appendix B, Irradiation Geometry.

^cSee Appendix C, Coronary Artery Nomenclature

^dMaximum coefficient of variation in percent.

+ Less than 0.001 mrad per R.

Table 5. RAO 15° Caudal 25° (left)
tissue dose (mrad) per 1-R exposure (free-in-air at skin-entrance plane)^a

Angulation^b of image receptor: transverse – 15°, sagittal – 25°. Field center^b: left ventricle.
SSD = 60 cm; SID = 90 cm; FOV_{Table} diameter at image receptor = 12 cm.

Arteries^c visualized: LM; prox, mid, dis Cx; M₁, M₂, M₃; Int; prox LAD; *ld*: LAV, LPLS, Crux, LPDA

HVL (mm Al)	2.5	4.0	5.5	2.0	3.5	5.0	Max. CV (%) ^d
Tissue	Male			Female			
Entrance skin in primary field	880	984	1040	836	960	1028	0.2
Brain	0.003	0.023	0.043	0.001	0.018	0.047	11.5
Thyroid	0.14	0.50	0.93	0.096	0.58	1.1	8.6
Thymus	1.7	4.8	7.2	1.2	4.6	8.0	2.4
Active bone marrow	4.3	7.9	10.7	3.7	8.2	12.0	0.1
Esophagus	14.4	32.0	44.8	11.5	33.6	51.6	0.7
Lung	25.1	40.1	49.2	23.2	42.4	54.8	0.1
Breast				1.4	5.0	8.2	0.6
Heart	22.3	47.8	66.3	17.2	47.7	72.2	0.2
Adrenal	2.3	6.3	9.2	1.7	6.2	10.3	2.4
Spleen	2.3	5.6	8.1	1.6	5.5	8.6	0.9
Pancreas	2.4	6.7	9.9	1.7	6.5	10.9	1.1
Stomach	1.9	4.9	7.1	1.4	4.8	8.0	0.9
Liver	0.92	2.8	4.3	0.66	2.8	5.1	0.6
Kidney	0.34	1.2	1.9	0.21	1.1	2.1	1.8
Colon	0.029	0.14	0.26	0.017	0.14	0.32	4.9
Small intestine	0.036	0.17	0.32	0.017	0.17	0.37	3.5
Ovary				0.001	0.047	0.072	61.7
Uterus				0.001	0.027	0.080	27.4
Urinary bladder	0.001	0.008	0.015	+	0.012	0.025	67.3
Testis	+	0.002	0.004				57.8

^aDivide table entries (mrad per R) by 25.8 to get SI units of (mGy per mC/kg exposure), by 0.876 to get (mGy per Gy air kerma).

^bSee Appendix B, Irradiation Geometry.

^cSee Appendix C, Coronary Artery Nomenclature

^dMaximum coefficient of variation in percent.

+ Less than 0.001 mrad per R.

Table 6. RAO 15° Cranial 25° (left)
tissue dose (mrad) per 1-R exposure (free-in-air at skin-entrance plane)^a

Angulation^b of image receptor: transverse - 15°, sagittal 25°. Field center^b: left ventricle.
SSD = 70 cm; SID = 95 cm; FOV_{Table} diameter at image receptor = 12 cm.

Arteries^c visualized: mid, dis LAD; D₂, D₃

HVL (mm Al)	2.5	4.0	5.5	2.0	3.5	5.0	Max. CV (%) ^d
Tissue	Male			Female			
Entrance skin in primary field	891	1000	1055	840	971	1041	0.2
Brain	0.001	0.014	0.034	0.001	0.014	0.034	17.5
Thyroid	0.097	0.38	0.67	0.065	0.38	0.81	13.5
Thymus	2.6	7.8	11.9	2.1	8.3	14.5	2.4
Active bone marrow	5.4	10.2	13.7	4.7	10.5	15.3	0.1
Esophagus	13.8	31.5	45.5	10.1	30.3	47.9	0.8
Lung	26.0	41.6	51.2	23.4	43.1	56.2	0.1
Breast				2.1	7.1	11.7	0.6
Heart	24.4	53.1	74.2	18.6	52.5	80.4	0.2
Adrenal	63.1	104	127	58.5	109	142	0.6
Spleen	10.9	22.0	28.9	8.8	22.5	32.0	0.4
Pancreas	8.5	19.6	27.3	6.3	19.5	29.9	0.6
Stomach	3.1	7.8	11.3	2.1	7.7	12.6	0.8
Liver	1.1	3.5	5.4	0.68	3.4	6.1	0.5
Kidney	3.9	8.3	11.1	3.1	8.4	12.5	0.6
Colon	0.082	0.34	0.59	0.048	0.34	0.71	3.1
Small intestine	0.11	0.45	0.79	0.059	0.43	0.90	2.0
Ovary				0.004	0.074	0.19	34.1
Uterus				0.005	0.083	0.18	16.0
Urinary bladder	0.004	0.020	0.055	0.001	0.026	0.056	44.1
Testis	+	+	0.004				100.0

^aDivide table entries (mrad per R) by 25.8 to get SI units of (mGy per mC/kg exposure), by 0.876 to get (mGy per Gy air kerma).

^bSee Appendix B, Irradiation Geometry.

^cSee Appendix C, Coronary Artery Nomenclature

^dMaximum coefficient of variation in percent.

+ Less than 0.001 mrad per R.

Table 7. Cranial 20° (right)
tissue dose (mrad) per 1-R exposure (free-in-air at skin-entrance plane)^a

Angulation^b of image receptor: transverse 0°, sagittal 20°. Field center^b: right ventricle.
SSD = 60 cm; SID = 90 cm; FOV_{Table} diameter at image receptor = 12 cm.

Arteries^c visualized: prox, mid, dis RCA; *rd*: RPDA, Crux, RPLS

HVL (mm Al)	2.5	4.0	5.5	2.0	3.5	5.0	Max. CV (%) ^d
Tissue	Male			Female			
Entrance skin in primary field	899	1007	1057	855	982	1049	0.2
Brain	0.001	0.006	0.014	0.000	0.005	0.016	25.2
Thyroid	0.025	0.14	0.28	0.016	0.18	0.37	20.4
Thymus	0.53	2.1	3.4	0.33	2.1	4.2	4.7
Active bone marrow	7.8	15.2	20.9	6.4	14.8	22.0	0.1
Esophagus	8.0	22.5	35.1	5.2	20.5	35.5	1.0
Lung	5.4	11.7	16.2	4.5	12.2	18.3	0.2
Breast				0.70	3.2	5.8	0.9
Heart	11.0	28.6	43.2	8.4	29.4	48.9	0.3
Adrenal	53.8	90.7	114	52.8	103	137	0.6
Spleen	2.6	6.9	9.9	1.9	6.7	10.9	0.8
Pancreas	4.7	12.8	19.1	3.3	12.6	21.1	0.8
Stomach	1.3	3.9	6.2	0.83	3.8	6.9	1.1
Liver	2.1	6.0	9.1	1.6	6.1	10.5	0.3
Kidney	2.5	6.2	8.8	1.9	6.1	9.8	0.6
Colon	0.054	0.28	0.51	0.033	0.27	0.61	3.3
Small intestine	0.072	0.36	0.66	0.040	0.34	0.76	2.2
Ovary				0.009	0.071	0.16	37.4
Uterus				0.004	0.067	0.16	19.4
Urinary bladder	0.004	0.019	0.032	0.001	0.021	0.053	50.5
Testis	+	0.001	0.006				95.5

^aDivide table entries (mrad per R) by 25.8 to get SI units of (mGy per mC/kg exposure), by 0.876 to get (mGy per Gy air kerma).

^bSee Appendix B, Irradiation Geometry.

^cSee Appendix C, Coronary Artery Nomenclature

^dMaximum coefficient of variation in percent.

+ Less than 0.001 mrad per R.

Table 8. LAO 45° Cranial 25° (left)
tissue dose (mrad) per 1-R exposure (free-in-air at skin-entrance plane)^a

Angulation^b of image receptor: transverse 45°, sagittal 25°. Field center^b: left ventricle.
SSD = 65 cm; SID = 90 cm; FOV_{Table} diameter at image receptor = 12 cm.

Arteries^c visualized: LM; prox, mid, dis LAD; S₁, S₂, S₃; D₁, D₂, D₃

HVL (mm Al)	2.5	4.0	5.5	2.0	3.5	5.0	Max. CV (%) ^d
Tissue	Male			Female			
Entrance skin in primary field	814	931	994	762	907	981	0.2
Brain	0.001	0.011	0.024	0.001	0.011	0.030	19.0
Thyroid	0.062	0.26	0.47	0.044	0.32	0.62	15.6
Thymus	0.98	3.3	5.2	0.68	3.4	6.4	3.6
Active bone marrow	5.2	10.5	14.5	4.4	10.5	15.9	0.1
Esophagus	8.7	22.0	32.9	5.7	20.2	33.8	1.1
Lung	15.3	26.6	34.2	13.2	27.2	37.4	0.2
Breast				0.76	3.5	6.4	0.9
Heart	17.2	38.1	54.0	13.6	39.0	60.2	0.3
Adrenal	72.0	122	155	63.7	126	170	0.6
Spleen	0.53	2.2	3.9	0.29	2.2	4.4	2.2
Pancreas	3.4	9.6	14.8	2.3	9.5	16.6	1.0
Stomach	0.62	2.3	4.0	0.37	2.3	4.5	1.8
Liver	18.6	33.1	42.5	16.1	34.3	47.2	0.1
Kidney	7.5	14.3	18.7	6.7	15.3	21.2	0.4
Colon	0.12	0.47	0.82	0.077	0.47	0.96	2.4
Small intestine	0.15	0.61	1.1	0.090	0.59	1.2	1.6
Ovary				0.011	0.088	0.29	23.9
Uterus				0.010	0.11	0.24	14.7
Urinary bladder	0.004	0.040	0.056	0.004	0.034	0.059	29.5
Testis	+	0.002	0.003				94.4

^aDivide table entries (mrad per R) by 25.8 to get SI units of (mGy per mC/kg exposure), by 0.876 to get (mGy per Gy air kerma).

^bSee Appendix B, Irradiation Geometry.

^cSee Appendix C, Coronary Artery Nomenclature

^dMaximum coefficient of variation in percent.

+ Less than 0.001 mrad per R.

Table 9. LAO 45° (left)
tissue dose (mrad) per 1-R exposure (free-in-air at skin-entrance plane)^a

Angulation^b of image receptor: transverse 45°, sagittal 0°. Field center^b: left ventricle.
SSD = 55 cm; SID = 90 cm; FOV_{Table} diameter at image receptor = 12 cm.

Arteries^c visualized: mid, dis Cx; M₂, M₃; *ld*: LAV, LPLS, Crux, LPDA; RCA

HVL (mm Al)	2.5	4.0	5.5	2.0	3.5	5.0	Max. CV (%) ^d
Tissue	Male			Female			
Entrance skin in primary field	823	929	985	775	905	973	0.2
Brain	0.002	0.012	0.025	0.001	0.011	0.027	13.8
Thyroid	0.077	0.33	0.57	0.055	0.34	0.70	10.6
Thymus	1.1	3.5	5.5	0.78	3.6	6.2	2.7
Active bone marrow	3.6	7.2	9.9	3.1	7.3	11.0	0.1
Esophagus	11.2	26.2	37.6	8.1	25.7	40.7	0.8
Lung	23.3	35.8	43.4	21.5	37.5	48.0	0.1
Breast				1.2	4.8	8.3	0.7
Heart	25.3	50.6	68.7	20.8	52.4	76.9	0.2
Adrenal	5.2	11.8	16.1	3.9	11.6	17.7	1.5
Spleen	0.37	1.4	2.5	0.20	1.4	2.8	2.2
Pancreas	1.5	4.4	6.8	0.94	4.3	7.6	1.3
Stomach	0.51	1.8	2.9	0.32	1.8	3.4	1.7
Liver	3.4	7.4	10.2	2.6	7.4	11.1	0.2
Kidney	0.59	1.8	2.7	0.40	1.7	3.0	1.2
Colon	0.029	0.14	0.26	0.018	0.15	0.32	4.2
Small intestine	0.036	0.18	0.33	0.019	0.17	0.38	3.0
Ovary				0.004	0.035	0.074	37.9
Uterus				0.003	0.034	0.084	23.9
Urinary bladder	0.002	0.011	0.025	+	0.007	0.028	48.3
Testis	+	0.003	0.003				67.2

^aDivide table entries (mrad per R) by 25.8 to get SI units of (mGy per mC/kg exposure), by 0.876 to get (mGy per Gy air kerma).

^bSee Appendix B, Irradiation Geometry.

^cSee Appendix C, Coronary Artery Nomenclature

^dMaximum coefficient of variation in percent.

+ Less than 0.001 mrad per R.

Table 10. RAO 10° Cranial 40° (left)
tissue dose (mrad) per 1-R exposure (free-in-air at skin-entrance plane)^a

Angulation^b of image receptor: transverse – 10°, sagittal 40°. Field center^b: left ventricle.
SSD = 60 cm; SID = 105 cm; FOV_{Table} diameter at image receptor = 12 cm.

Arteries^c visualized: prox, mid, dis LAD; D₁, D₂, D₃; S₁, S₂, S₃

HVL (mm Al)	2.5	4.0	5.5	2.0	3.5	5.0	Max. CV (%) ^d
Tissue	Male			Female			
Entrance skin in primary field	843	951	1007	796	929	993	0.2
Brain	0.001	0.007	0.015	+	0.005	0.018	18.6
Thyroid	0.034	0.16	0.32	0.020	0.15	0.38	17.2
Thymus	1.3	4.0	6.2	0.92	4.2	7.6	3.0
Active bone marrow	3.4	6.5	8.8	2.9	6.6	9.7	0.1
Esophagus	5.0	12.9	19.4	3.5	12.2	20.7	1.0
Lung	6.4	12.2	16.2	5.4	12.6	18.0	0.2
Breast				0.40	1.9	3.4	0.9
Heart	8.0	19.6	28.9	5.9	19.9	32.3	0.3
Adrenal	88.9	145	181	75.3	142	188	0.4
Spleen	8.4	17.4	22.9	6.6	17.5	25.1	0.4
Pancreas	7.6	17.3	23.8	5.6	17.0	26.0	0.5
Stomach	2.0	5.3	7.8	1.4	5.2	8.6	0.8
Liver	0.64	2.2	3.5	0.40	2.1	4.0	0.5
Kidney	11.2	19.0	23.7	10.7	21.1	27.7	0.3
Colon	0.095	0.37	0.61	0.064	0.38	0.74	2.1
Small intestine	0.14	0.53	0.89	0.085	0.50	0.99	1.3
Ovary				0.015	0.10	0.26	24.9
Uterus				0.008	0.086	0.20	12.8
Urinary bladder	0.004	0.027	0.046	0.001	0.026	0.057	27.7
Testis	+	+	0.002				79.7

^a Divide table entries (mrad per R) by 25.8 to get SI units of (mGy per mC/kg exposure), by 0.876 to get (mGy per Gy air kerma).

^b See Appendix B, Irradiation Geometry.

^c See Appendix C, Coronary Artery Nomenclature

^d Maximum coefficient of variation in percent.

+ Less than 0.001 mrad per R.

Table 11. Anterior View (left)
tissue dose (mrad) per 1-R exposure (free-in-air at skin-entrance plane)^a

Angulation^b of image receptor: transverse 0°, sagittal 0°. Field center^b: left ventricle.
SSD = 50 cm; SID = 90 cm; FOV_{Table} diameter at image receptor = 23 cm.

Arteries^c visualized: dis Cx; D₃; dis LAD

HVL (mm Al)	2.5	4.0	5.5	2.0	3.5	5.0	Max. CV (%) ^d
Tissue	Male			Female			
Entrance skin in primary field	932	1049	1107	882	1027	1101	0.2
Brain	0.005	0.033	0.075	0.003	0.031	0.083	14.7
Thyroid	0.20	0.86	1.5	0.13	0.95	2.0	12.0
Thymus	3.4	10.1	16.9	2.4	11.1	19.8	2.9
Active bone marrow	15.1	28.5	38.4	12.6	28.0	40.8	0.1
Esophagus	23.4	58.9	88.4	16.1	56.2	92.5	0.9
Lung	53.4	85.5	106	50.4	92.0	120	0.1
Breast				10.2	27.9	42.5	0.4
Heart	29.3	70.6	103	21.5	69.4	111	0.3
Adrenal	35.1	64.0	82.3	34.2	72.1	99.3	1.1
Spleen	7.6	17.8	24.5	5.9	17.9	27.6	0.8
Pancreas	8.9	22.4	32.8	6.6	22.9	37.0	0.9
Stomach	5.5	13.4	19.4	4.2	14.1	22.8	0.9
Liver	2.8	8.5	13.1	2.1	8.8	15.6	0.5
Kidney	2.0	5.7	8.8	1.5	5.9	9.9	1.1
Colon	0.088	0.41	0.78	0.048	0.45	0.95	4.4
Small intestine	0.11	0.52	0.96	0.058	0.53	1.2	2.9
Ovary				0.007	0.093	0.27	51.3
Uterus				0.006	0.082	0.21	25.6
Urinary bladder	0.002	0.018	0.068	0.002	0.033	0.087	67.7
Testis	+	0.008	0.003				68.4

^aDivide table entries (mrad per R) by 25.8 to get SI units of (mGy per mC/kg exposure), by 0.876 to get (mGy per Gy air kerma).

^bSee Appendix B, Irradiation Geometry.

^cSee Appendix C, Coronary Artery Nomenclature

^dMaximum coefficient of variation in percent.

+ Less than 0.001 mrad per R.

Table 12. Nominal Conversion Coefficients
tissue dose (mrad) per 1-R exposure (free-in-air at skin-entrance plane)^a

Average values for all angulations of image receptor.*
SSD = 60 cm; SID = 90 cm; FOV_{Table} diameter at image receptor = 14 cm.

HVL (mm Al)	2.5	4.0	5.5	2.0	3.5	5.0	Max. CV _{nom} (%) ^b
Tissue	Male			Female			
Entrance skin in primary field	880	980	1030	830	960	1020	5
Brain	0.002	0.017	0.036	0.001	0.015	0.039	60
Thyroid	0.11	0.44	0.75	0.066	0.46	0.93	50
Thymus	1.9	5.7	8.7	1.4	5.9	10	50
Active bone marrow	5.4	10	14	4.6	10	15	70
Esophagus	12	29	41	9.3	28	45	60
Lung	30	46	57	27	48	63	70
Breast				2.6	8.2	13	110
Heart	26	55	76	20	55	83	50
Adrenal	31	54	69	28	56	76	100
Spleen	4.3	9.6	13	3.3	9.6	15	100
Pancreas	4.7	12	17	3.4	12	19	60
Stomach	2.1	5.5	8.2	1.5	5.5	9.2	90
Liver	3.8	8.5	12	3.0	8.6	13	150
Kidney	2.8	5.9	8.1	2.4	6.2	9.2	140
Colon	0.062	0.27	0.49	0.037	0.28	0.59	50
Small intestine	0.080	0.35	0.63	0.044	0.34	0.72	60
Ovary				0.006	0.066	0.17	70
Uterus				0.005	0.062	0.15	60
Urinary bladder	0.002	0.018	0.039	0.001	0.020	0.047	80
Testis	+	0.002	0.003				150

^aA tabulated nominal conversion coefficient is the arithmetic mean of the respective entries of Tables 1 through 11.

^bMax. CV_{nom} refers to the maximum amongst the (six) coefficients of variation for a particular tissue. Here CV_{nom} is the ratio (in percent) of the standard deviation to the nominal conversion coefficient (for a particular tissue and HVL). The standard deviation refers to the distribution of entries in Tables 1 through 11 from which a Table-12 mean is calculated as a nominal value (for a particular tissue and HVL).

+ Less than 0.001 mrad absorbed dose per 1 R exposure.

APPENDIX A. Phantom Anthropometric Characteristics

Table A-1. Dimensions (cm) and Weight (kg) of Reference Male (ADAM) and Female (EVA) Adult Phantoms (5)

	Male (ADAM)	Female (EVA)
Height	170.0	160.0
Head, anterior-posterior thickness	20.0	18.8
side-to-side width	16.0	15.0
circumference	56.7	53.3
Thorax and abdomen, anterior-posterior thickness	20.0	18.8, 23.9 ^a
side-to-side width ^b	40.0	37.6
circumference ^b	96.9	91.1
Weight	70.5	59.2

^a18.8 cm from back to chest wall; 23.9 cm from back to nipple of breast.

^bThe torsos of Adam and Eva are elliptical cylinders which incorporate arms at the sides. Hence the "side-to-side width" and "circumference" include the arms as part of the dimensions specified.

APPENDIX B. Irradiation Geometry

Views are described from the perspective of an observer at the image receptor looking at the phantom. In Tables 1-11 the "transverse angulation" is the angle between the table perpendicular and the geometric projection of the central ray in the transverse plane. A negative angle corresponds to an oblique view of the phantom's right anterior and designates an "RAO" view. A positive angle corresponds to a view of the phantom's left anterior and designates an "LAO" view. The "sagittal angulation" is the angle between the table perpendicular and the geometric projection of the central ray in the sagittal plane. A negative value corresponds to a view of the phantom from a caudal perspective, a positive value from a cranial perspective.

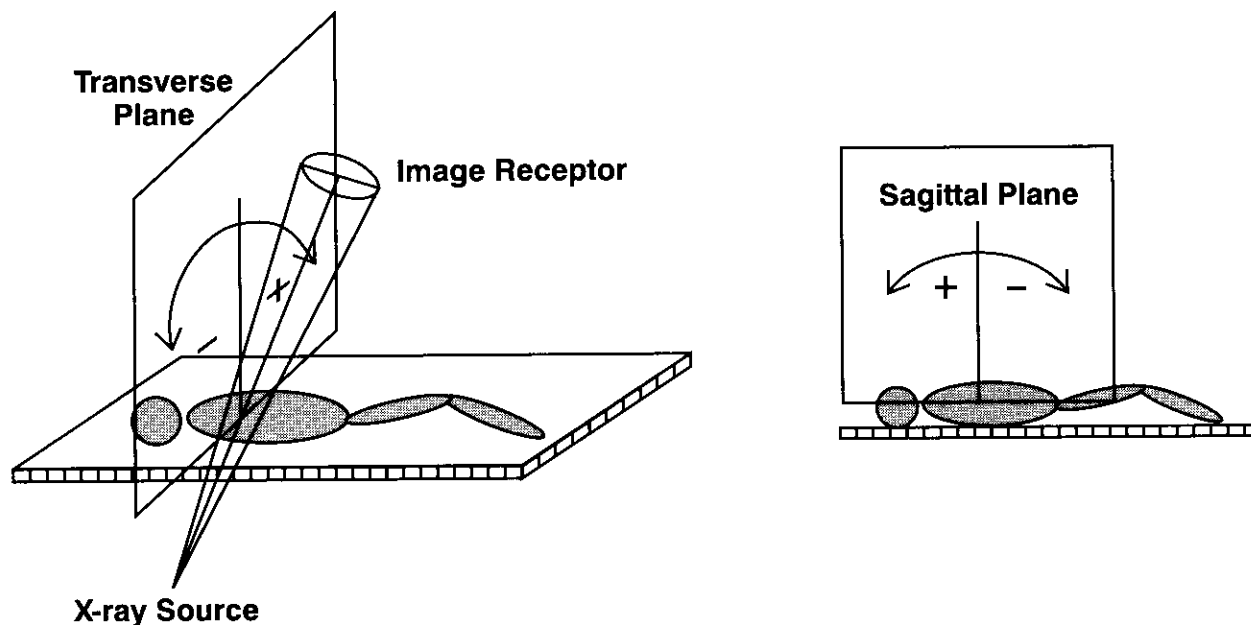


Figure B-1. Sign conventions for transverse- and sagittal-plane angulations.

For each of the x-ray fields simulated, the central ray follows a trajectory through a "field center" within each phantom that is either the left or right ventricle center, as specified in Tables 1-11. The following coordinates locate the ventricle centers:

Table B-1. Coordinates^a (cm) of Ventricle Centers

Phantom Gender	Left			Right		
	x_l	y_l	z_l	x_r	y_r	z_r
Male (ADAM)	2.83	-2.03	48.43	0.72	-6.56	48.43
Female (EVA)	2.66	-1.91	45.52	0.68	-6.17	45.52

^aIn the phantom coordinate system (5), +x is the distance from the midsagittal plane toward the phantom's left; +y is the distance from the midfrontal plane toward the phantom's posterior; +z is the distance from the base of the torso toward the vertex (located at $z = 94$ cm for ADAM, 89 cm for EVA). The origin of the coordinate system is the point intersected by the midsagittal plane, the midfrontal plane, and the horizontal plane at the base of the torso.

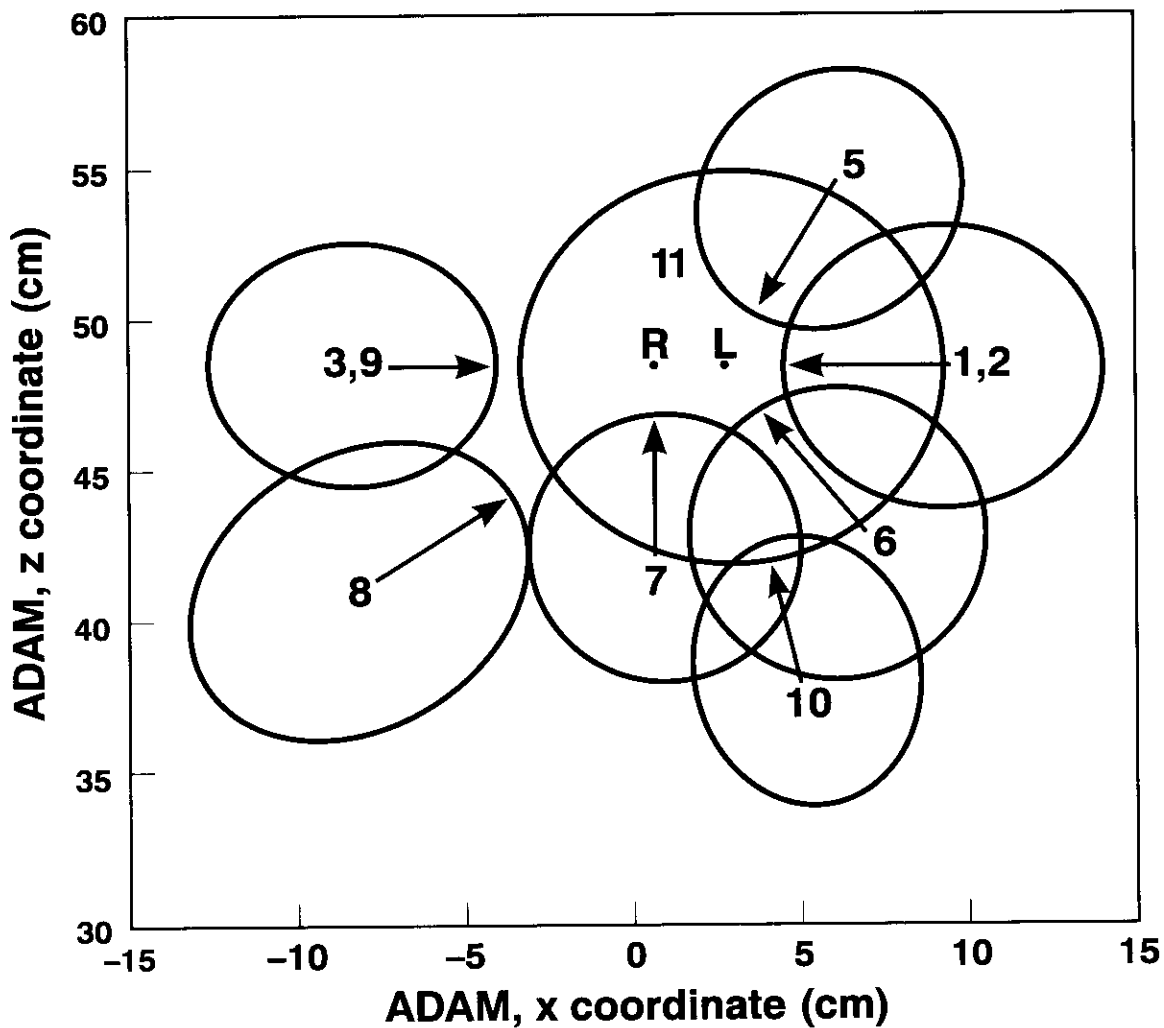


Figure B-2. Projections of the intersections of various x-ray fields (page iv) with the skin-entrance planes of the male phantom ADAM.

Figure B-2 is depicted from the perspective of an observer looking toward the anterior of the phantom; x-rays originate posterior to the phantom. The xz-plane shown is parallel to the tabletop plane. Each elliptical area is a geometric projection of an x-ray field intersection of a skin-entrance plane. A skin-entrance plane is the plane tangent to the phantom surface at the point where the central ray intercepts the posterior skin surface. Arrows indicate central-ray trajectories of each field toward the right (R) or left (L) ventricle center (Table B-1). X-ray fields are labeled by the Handbook Table numbers appearing within the ellipses. The field associated with the LLAT view (Table 4) is not represented in this figure.

In the phantom coordinate system (5), +x is the distance from the midsagittal plane toward the phantom's left; +y is the distance from the midfrontal plane toward the phantom's posterior; +z is the distance from the base of the torso toward the vertex, located at $z = +94$ cm for ADAM. The origin of the coordinate system is the point intersected by the midsagittal plane, the midfrontal plane, and the horizontal plane at the base of the torso. For the ensemble of elliptical projections shown, values of the y coordinate range from +7.5 cm to +10.4 cm, corresponding to the phantom posterior.

APPENDIX C. Coronary Artery Nomenclature

The names of the coronary arteries used in this handbook are adopted from the anatomy nomenclature described in the Coronary Artery Surgery Study (CASS) (13) and extended in the Bypass Angioplasty Revascularization Investigation (BARI) (14). Table C-1 defines the abbreviations cited in Tables 1-11 in terms of this nomenclature, and it also lists the corresponding arterial segment identification numbers as given in references (13) and (14). Major arteries are depicted in Figure C-1.

Table C-1. Abbreviations, Terminology, and CASS/BARI Identification Numbers of Coronary Artery System

Abbreviation	Terminology	Reference (13,14) Identification Numbers
Crux	posteroatrioventricular groove segment	5
Cx	circumflex artery	18 (proximal), 19 (middle), 19a (distal)
D₁, D₂, D₃	first, second, third diagonals	15, 16, 29, respectively
dis	distal	
Int	ramus intermedius	28
LAD	left anterior descending artery	12 (proximal), 13 (middle), 14 (distal)
LAV	left atrioventricular groove segment, circumflex artery continuation	23
ld	left-dominant coronary circulation	
LM	left main coronary artery	11
LPDA	left posterior descending artery	27 (present for left dominance)
LPLS	left posterolateral segments	24 (first), 25 (second), 26 (third) (present for mixed or left dominance)
M₁, M₂, M₃	first, second, third obtuse marginals	20, 21, 22, respectively
mid	middle	
prox	proximal	
RCA	right coronary artery	1 (proximal), 2 (middle), 3 (distal)
rd	right-dominant coronary circulation	
RPDA	right posterior descending artery	4 (present for right dominance)
RPLS	right posterolateral segments	6 (first), 7 (second), 8 (third) (present for right dominance)
S₁, S₂, S₃	first, second, third anterior septals	17

Major Coronary Artery Segments

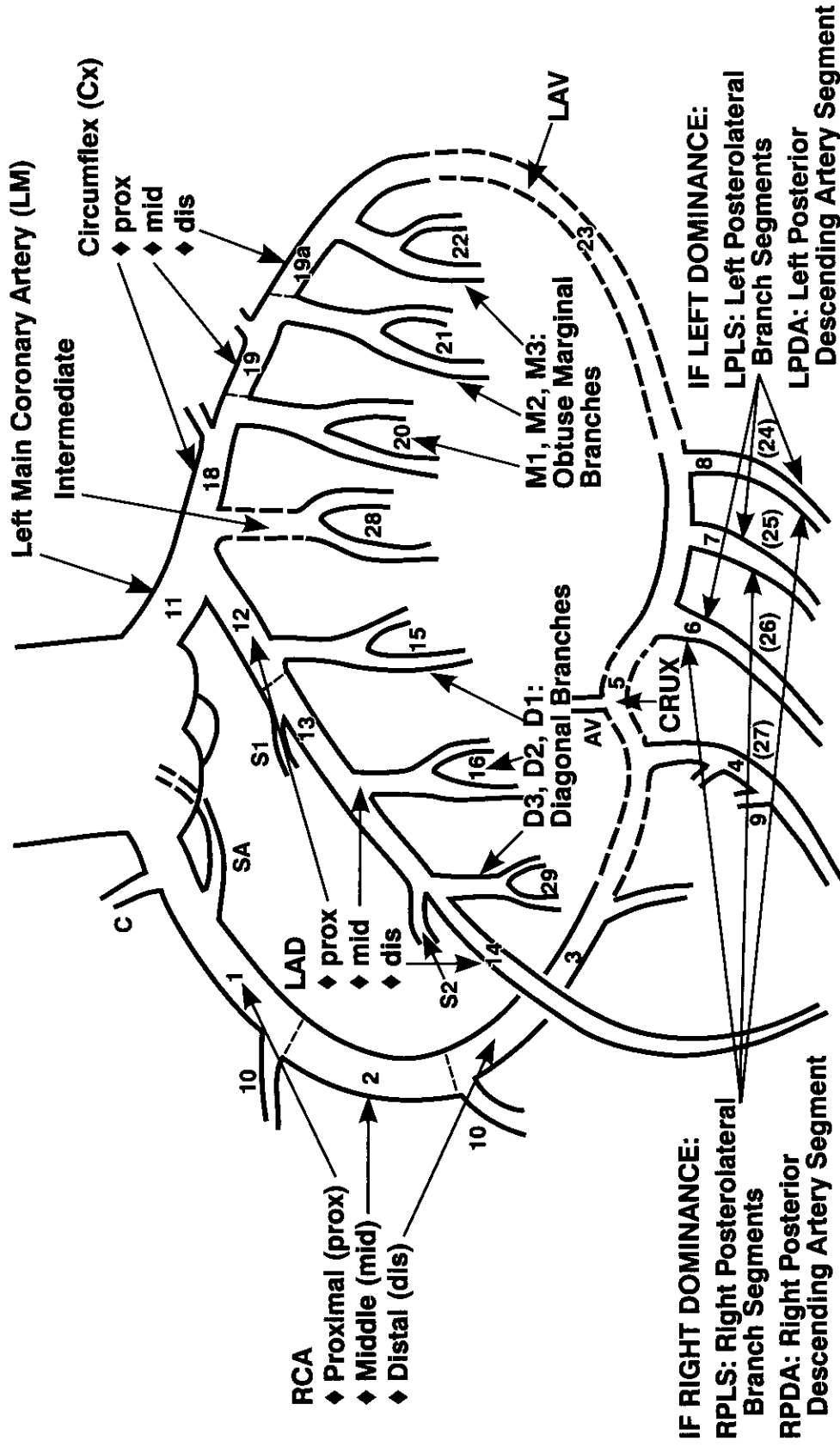


Figure C-1. The major coronary artery segments following the nomenclature of CASS (13) and BARI (14).

APPENDIX D. Sample Analysis of Fluoroscopic and Cineangiographic Examination of the Coronary Arteries

Method A: View-by-View Analysis of an Examination

Tissue doses from a broad range of examinations of the coronary arteries may be estimated on the basis of the 11 views simulated for this Handbook. Clinically representative examinations may be analyzed from videotape and film records. Videotape records may be dubbed with a time code as well as with complementary information about image-receptor angulations, field-center location and FOV diameter, operating tube voltage, current, and, as warranted, pulse width, frame rate, and exposure intervals for all continuous and pulsed fluoroscopic and cineangiographic modes. The records may then be analyzed in terms of fluoroscopic scan segments and associated cineangiographic films whose views most closely correspond to those simulated for Tables 1 through 11.

As an example, Tables D-1 through D-4 illustrate such an analysis adapted from an actual left-heart study of an adult male (15). The study entailed a left ventriculogram (LV) done in biplanar-mode (i.e., with simultaneous image acquisition by two x-ray systems at complementary angles) followed by left (L) and right (R) coronary angiography (CA). The specific fluoroscopic exposure times, number of cine frames used, and associated examination sequence and technique factors were all recorded in (15).

Tables D-1 through D-4 follow the instructions for **Method A: View-by-View Analysis of an Examination**, and they correspond to four phases in the evaluation of tissue doses — (1) association of Handbook Table views with examination views, (2) evaluation of fluoroscopic and cineangiographic exposure for each of the Table views of the examination, (3) HVL selection and FOV correction for each of the Table views, and (4) selection of Table conversion coefficients and evaluation of tissue doses.

Table D-1. Adult Male LV/LCA/RCA — Examination Sequence

Examination Parameters ^a (15)							Applicable Handbook Table ^c
Fluoro Time (min); No. of Cine Frames	View	Voltage (kVp)	Current (mA); Pulse width (ms) ^b	SSD (cm)	SID (cm)	FOV diam ^c (cm)	
LV preparation (x-ray sys. 1)							
a 3.0 min	Anterior	85	4.0 mA	46	92	22.9	11
b 1.6 min	Anterior	75	3.5 mA	46	92	22.9	11
c 1.9 min	LAO 37°	76	4.5 mA	53	94	22.9	3
d 1.1 min	RAO 38°	90	5.0 mA	53	94	15.2	1
e 0.6 min	LAO 44°	90	4.0 mA	53	94	15.2	9
f 0.5 min	Anterior	80	4.0 mA	53	96	22.9	11
g 4.0 min	LAO 41°	80	5.0 mA	53	96	22.9	9
LV (x-ray sys. 1)							
h 1.6 min	RAO 30°	76	2.0 mA	56	94	22.9	1
i 0.6 min; 240 frames	RAO 30°	75; 70	2.0 mA; 2.0 ms	56	94	22.9	1
(x-ray sys. 2)							
j 0.8 min	LAO 60°	75	12.0 mA	56	111	22.9	9
k 1.0 min; 240 frames	LAO 60°	100; 85	5.0 mA; 5.3 ms	56	111	22.9	9

Table D-1. (continued)

Examination Parameters ^a (15)							Applicable Handbook Table ^d
Fluoro Time (min); No. of Cine Frames	View	Voltage (kVp)	Current (mA); Pulse width (ms) ^b	SSD (cm)	SID (cm)	FOV diam ^c (cm)	
LCA (x-ray sys. 1)							
l 0.4 min	Anterior	76	2.0 mA	56	91	22.9	11
m 0.3 min; <i>106 frames</i>	LAO 40°	102; <i>75</i>	3.5 mA; <i>5.9 ms</i>	56	90	15.2	9
n 0.2 min; <i>126 frames</i>	{LAO 41° Cran 19°}	120; <i>97</i>	4.0 mA; <i>10.0 ms</i>	66	103	15.2	8
o 0.1 min; <i>138 frames</i>	Cranial 38°	120; <i>91</i>	4.0 mA; <i>10.0 ms</i>	73	113	15.2	10
p 0.1 min; <i>137 frames</i>	RAO 31°	120; <i>75</i>	4.0 mA; <i>6.7 ms</i>	73	102	15.2	1
q 0.1 min; <i>147 frames</i>	{RAO 42° Caud 15°}	120; <i>84</i>	4.0 mA; <i>7.3 ms</i>	73	105	15.2	5
r 0.2 min; <i>98 frames</i>	{LAO 22° Caud 30°}	120; <i>94</i>	4.0 mA; <i>7.6 ms</i>	73	102	15.2	3
RCA (x-ray sys. 1)							
s 0.2 min	Anterior	76	3.5 mA	59	102	22.9	11
t 0.6 min; <i>130 frames</i>	LAO 39°	120; <i>75</i>	4.0 mA; <i>7.0 ms</i>	59	100	15.2	9
u 0.2 min; <i>131 frames</i>	{LAO 45° Cran 19°}	120; <i>108</i>	4.0 mA; <i>10.0 ms</i>	59	105	15.2	8
v 0.1 min; <i>118 frames</i>	{RAO 36° Cran 20°}	120; <i>101</i>	4.0 mA; <i>7.3 ms</i>	59	103	15.2	6
w 0.1 min	Cranial 40°	120	4.0 mA	73	113	15.2	10
x 0.8 min	LAO 41°	120	4.0 mA	59	105	15.2	9
y 0.3 min	Anterior	76	3.5 mA	53	96	22.9	11
z 0.9 min	Anterior	110	3.5 mA	53	96	15.2	11
aa 0.4 min; <i>124 frames</i>	Cranial 42°	120; <i>114</i>	4.0 mA; <i>10.0 ms</i>	79	114	15.2	10

^aThe chronological sequence of examination segments is represented alphabetically. For any particular segment, the cine mode was pulsed at rate of 1800 frames/min and had the same angulations, SSD, SID, and FOV diameter as listed for the fluoro mode (15). Values for other cineangiographic parameters are indicated in *italics*. Cineangiography was not done for each examination segment.

^bTube current values refer to fluoroscopic mode only; pulse width values refer to cineangiographic mode only (15).

^cField-of-view diameter at the image-receptor plane (15).

^dSee Method A, Instruction 1.

For each of the applicable Tables enumerated in Table D-1, the x-ray system(s) radiation output needs to be evaluated separately for the fluoroscopic and cineangiographic modes of operation. For reference planes located at observed SSDs, one determines free-in-air exposures. Continuing with the preceding example of analysis of an LV/LCA/RCA examination as recorded in (15), Table D-2 illustrates evaluations of radiation output for each group of examination segments associated with a view.

Table D-2. Adult Male LV/LCA/RCA — Examination Radiation Output

Applicable Handbook Table ^a	Examination Segment Group ^a (fluoro)	SSD ^b (cm)	Voltage ^b (kVp)	Group HVL ^c (mm Al)	Current ^b (mA)	Fluoro Exposure Rate ^d (R/min)	Fluoro Exposure Time ^e (min)	Fluoro Exposure ^f (R)
1	{d,h,i,p}	56	82	3.3	3.0	3.7	3.4	13
3	{c,r}	55	80	3.2	4.5	5.5	2.1	11
5	q	73	120	5.1	4.0	5.5	0.1	0.5
6	v	59	120	5.1	4.0	8.4	0.1	0.8
8	{n,u}	63	120	5.1	4.0	9.0	0.4	3.6
9	{e,g,j,k,m,t,x}	55	90	3.5	5.4	7.7	8.1	62
10	{o,w,aa}	77	120	5.1	4.0	4.9	0.6	3.0
11	{a,b,f,l,s,y,z}	49	84	3.4	3.7	6.2	6.9	43
Applicable Handbook Table ^a	Examination Segment Group ^a (cine)	SSD ^b (cm)	Voltage ^b (kVp)	Group HVL ^c (mm Al)	Pulse Width ^b (ms)	Cine Exposure Rate ^g (R/min)	Number of Cine Frames ^h	Cine Exposure ⁱ (R)
1	{i,p}	62	72	2.8	3.6	26	367	5.3
3	r	73	94	3.9	7.6	45	98	2.4
5	q	73	84	3.4	7.3	40	147	3.3
6	v	59	101	4.2	7.3	70	118	4.6
8	{n,u}	62	103	4.3	10.0	85	257	12
9	{k,m,t}	57	80	3.0	5.9	56	476	15
10	{o,aa}	76	102	4.3	10.0	57	262	8.4

^aFor each group, examination segments share a common view and are associated with an applicable Table. See Table D-1.

^bAn entry is the average value determined for the group of examination segments, each contribution (Table D-1) weighted by segment exposure time if fluoroscopic or by the number of cine frames in the segment if cineangiographic.

^cAn HVL of the examination segment group is evaluated according to the voltage (Table D-2 column 4) for the group and calibrations (15) of HVL versus tube voltage.

^dThe fluoroscopic exposure rate of the examination segment group is evaluated according to the voltage (Table D-2 column 4) for the group and calibrations (15) of exposure rate versus tube voltage. The evaluation includes an inverse-square-law correction to account for the group SSD (Table D-2 column 3) and an adjustment for group current (Table D-2 column 6).

^eFor each group of examination segments, an entry is the sum of the exposure times (Table D-1) if fluoroscopic or the sum of the numbers of cine frames (Table D-1) if cineangiographic.

^fExposure (free-in-air) at SSD, evaluated as the product of the fluoroscopic exposure rate (Table D-2 column 7) and exposure time (Table D-2 column 8).

^gThe cine exposure rate of the examination segment group is evaluated according to the voltage (Table D-2 column 4) for the group and calibrations (15) of exposure rate versus tube voltage. The evaluation includes an inverse-square-law correction to account for the group SSD (Table D-2 column 3) and an adjustment for group pulse width (Table D-2 column 6).

^hExposure (free-in-air) at SSD, product of cine exposure rate (Table D-2 column 7, per 1800 frames/min) and number of frames (Table D-2 column 8).

In order to select appropriate conversion coefficients, HVLs applicable to tabulated entries of the coefficients need to be designated for each Table. Applicable HVLs are those HVLs in the Tables which most closely represent the average HVL of the group of examination segments associated with a Table. Furthermore, one needs to apply a correction factor when a clinical field-of-view diameter (FOV_{group}) for a group of examination segments is different by more than $\pm 20\%$ from FOV_{Table} , the diameter specified in each Table. Table D-3 illustrates the determination of applicable HVLs and FOV correction factors.

Table D-3. Adult Male LV/LCA/RCA – HVLs, FOV Corrections Applicable to Evaluate Tissue Doses

Applicable Hand-book Table ^a	Examination Segment Group ^a	Group HVL ^b (mm Al)	Applicable HVL ^c (mm Al)	FOV_{group} ^d diam (cm)	FOV_{Table} ^e diam (cm)	FOV Correction Factor ^f
1	fluoro {d,h,i,p}	3.3	4.0	20.2	14	2.1
	cine {i,p}	2.8	2.5	20.2	14	2.1
3	fluoro {c,r}	3.2	2.5	22.2	12	3.4
	cine r	3.9	4.0	15.2	12	1.6
5	fluoro q	5.1	5.5	15.2	12	1.6
	cine q	3.4	4.0	15.2	12	1.6
6	fluoro v	5.1	5.5	15.2	12	1.6
	cine v	4.2	4.0	15.2	12	1.6
8	fluoro {n,u}	5.1	5.5	15.2	12	1.6
	cine {n,u}	4.3	4.0	15.2	12	1.6
9	fluoro {e,g,j,k,m,t,x}	3.5	4.0	20.7	12	3.0
	cine {k,m,t}	3.0	2.5	19.2	12	2.5
10	fluoro {o,w,aa}	5.1	5.5	15.2	12	1.6
	cine {o,aa}	4.3	4.0	15.2	12	1.6
11	fluoro {a,b,f,l,s,y,z}	3.4	4.0	21.9	23	not applicable

^aFor each group, examination segments share a common view and are associated with an applicable Table. See Table D-1.

^bFrom Table D-2.

^cHVL applicable in the selection of conversion coefficients from the Tables. For examinations of males, applicable HVLs are 2.5, 4.0, and 5.5 mm Al; for females, applicable HVLs are 2.0, 3.5, 5.0 mm Al. In this example, the examination is of a male. The specific values selected are those that most closely represent respective group HVLs.

^dAn entry is the average value determined for the group of examination segments, each contribution (Table D-1) weighted by segment exposure time if fluoroscopic or by the number of cine frames in the segment if cineangiographic.

^e FOV_{Table} is the diameter specified in the applicable Table for the field of view at the image-receptor plane. Its value defines the size of the x-ray field in the Monte Carlo simulation generating the Table conversion coefficients.

^fWhen FOV_{group} differs from FOV_{Table} by more than $\pm 20\%$, a correction factor is applicable in the evaluation of tissue dose for all tissue except the Entrance Skin in the Primary Field (ESPF). The applicable FOV correction factor = $(FOV_{group}/FOV_{Table})^2$. No FOV correction factor is to be applied in evaluation of dose in ESPF.

For each view of the examination, conversion coefficients are selected according to applicable HVL. For tissues other than the Entrance Skin in the Primary Field (ESPF), the dose is evaluated as the product of the conversion coefficient, the exposure, and the FOV correction factor (when FOV correction is applicable). For ESPF, the dose is evaluated as the product of the conversion coefficient and the exposure. These evaluations are illustrated in Table D-4.

Table D-4. Adult Male LV/LCA/RCA — Absorbed Doses to Entrance Skin in Primary Field (ESPF), Active Bone Marrow (ABM) and Lung Tissue

Applicable Handbook Table ^a	Examination Segment Group ^a	Applicable HVL ^b (mm Al)	Tissue Dose (mrad) per 1-R Exposure ^c			Exposure ^d (R)	FOV Correction Factor ^e	Tissue Dose ^f (rad)		
			ESPF	ABM	Lung			ESPF	ABM	Lung
1	fluoro {d,h,i,p}	4.0	981	8.3	81.7	13	2.1	13	0.23	2.2
	cine {i,p}	2.5	880	4.6	55.7	5.3	2.1	4.7	0.05	0.62
	view subtotal					18		18	0.28	2.8
3	fluoro {c,r}	2.5	874	3.4	37.9	11	3.4	9.6	0.13	1.4
	cine r	4.0	974	6.2	55.5	2.4	1.6	2.3	0.02	0.21
	view subtotal					13		11.9	0.15	1.6
5	fluoro q	5.5	1040	10.7	49.2	0.5	1.6	0.5	0.01	0.04
	cine q	4.0	984	7.9	40.1	3.3	1.6	3.2	0.04	0.21
	view subtotal					3.8		3.7	0.05	0.25
6	fluoro v	5.5	1055	13.7	51.2	0.8	1.6	0.8	0.02	0.07
	cine v	4.0	1000	10.2	41.6	4.6	1.6	4.6	0.07	0.31
	view subtotal					5.4		5.4	0.09	0.38
8	fluoro {n,u}	5.5	99	14.5	34.2	3.6	1.6	3.6	0.08	0.20
	cine {n,u}	4.0	931	10.5	26.6	12	1.6	11	0.20	0.51
	view subtotal					16		15	0.28	0.71
9	fluoro {e,g,j,k,m,t,x}	4.0	929	7.2	35.8	62	3.0	58	1.3	6.7
	cine {k,m,t}	2.5	823	3.6	23.3	15	2.5	12	0.14	0.87
	view subtotal					77		70	1.4	7.6

Table D-4. (continued)

Applicable Handbook Table ^a	Examination Segment Group ^a	Applicable HVL ^b (mm Al)	Tissue Dose (mrad) per 1-R Exposure ^c			Exposure ^d (R)	FOV Correction Factor ^e	Tissue Dose ^f (rad)		
			ESPF	ABM	Lung			ESPF	ABM	Lung
10	fluoro {o,w,aa}	5.5	1007	8.8	16.2	3.0	1.6	3.0	0.04	0.08
	cine {o,aa}	4.0	951	6.5	12.2	8.4	1.6	8.0	0.09	0.16
	view subtotal					11.4		11.0	0.13	0.24
11	fluoro {a,b,f,l,s,y,z}	4.0	1049	28.5	85.5	43	n/a	45	1.2	3.7
	Fluoroscopic subtotal					g		g	3.1	14.4
	Cineangiographic subtotal					g		g	0.6	2.9
	Examination total					g		g	3.7	17.3

^aFor each group, examination segments share a common view and are associated with an applicable Table. See Table D-1.

^bFrom Table D-3.

^cEntries excerpted from Tables 1 through 11, as specified according to applicable Table.

^dFrom Table D-2.

^eFrom Table D-3. When FOV_{group} diameter differs by less than $\pm 20\%$ from the FOV_{Table} diameter, no correction is applicable, and the entry is denoted "n/a." When applicable, the FOV correction factor refers to the evaluation of doses in all tissues except for the entrance skin in the primary field (ESPF).

^fFor tissues other than ESPF, the dose is the product of the tissue dose per 1-R exposure (free-in-air at the skin-entrance plane), exposure, and the FOV correction factor. Dose in ESPF is the product of the ESPF dose per 1-R exposure (free-in-air at the skin-entrance plane) and the exposure.

^gSubtotals and totals are not relevant for noncumulative quantities. Exposures for the different views of the examination entail different irradiation geometries and are not cumulative at a unique location; a different region of entrance skin tissue is exposed for each different view, and ESPF doses are cumulative only to the limited extent that entrance skin sites share a common locus of exposure in the various primary fields (Appendix B, Figure B-2).

APPENDIX E. Sample Analysis of Fluoroscopic and Cineangiographic Examination of the Coronary Arteries

Method B: Nominal Analysis of an Examination

One can apply an alternative method to evaluate nominal tissue doses. Table E-1 illustrates how nominal tissue doses can be evaluated without the detailed information required for Method A. Table E-1 follows the instructions for **Method B: Nominal Analysis of an Examination**. Method B is illustrated in Table E-1 for the same examination exemplified in Tables D-1 through D-4.

Table E-1. Adult Male LV/LCA/RCA — Absorbed Doses to ESPF, ABM and Lung Tissue by Nominal Analysis

Parameters for Entire Exam		Nominal Values ^a
nominal half-value layer (HVL)		3.6 mm Al
total exposure (free-in-air) at all skin-entrance planes		190 R
FOV _{nominal} diameter at image-receptor plane		20 cm
highest cumulative entrance exposure at any single skin location		90 R
FOV correction factor: $(20/14)^2$		2.0
Tissue	Tissue Dose (mrad) per 1-R Exposure ^b	Nominal ^a Tissue Dose ^c (rad) for Entire Examination
Entrance skin in primary field (ESPF) ^d	950	86 ^d
Active bone marrow (ABM)	8.8	3.3
Lung	42	16

^aSee text below.

^bConversion coefficients have been interpolated in this particular example for 3.6 mm Al HVL from Handbook Table 12 entries corresponding to 2.5 and 4.0 mm Al, respectively by tissue.

^cFor all tissues except ESPF, tissue dose is a product of the interpolated conversion coefficient, total exposure (190 R in this example), and the FOV correction factor (2.0 in this example).

^dThe dose in ESPF is the largest amount for any single skin location. It is the product of the interpolated conversion coefficient (950 mrad/R in this example) and the highest cumulative entrance exposure (90 R in this example) at any single skin location.

The principal point of Table E-1 is to illustrate how to *apply* Method B after the nominal HVL, total exposure, FOV_{nominal} diameter, and highest cumulative entrance exposure at any single skin location have been estimated by a user. Table E-1 does not prescribe *how* to determine nominal HVL, total exposure, FOV_{nominal} diameter, and highest cumulative entrance exposure at any single skin location.

Authors' comments:

1. In this particular example, the values tabulated to represent "nominal" HVL and the FOV_{nominal} diameter are exposure-weighted averages of the parameters specified view-by-view in Table D-2. The total exposure value 190 R is a sum of the exposures for each view. Similarly, the "nominal" estimate 90 R for the highest cumulative entrance exposure at any single skin location is a sum of the 77 R exposure associated with the LAO 45° view (Table 9) and the 13 R exposure associated with the LAO 30° view (Table 3). The latter views share a common locus of skin irradiation (Figure B-2).

Because the values selected for the "nominal" examination parameters are in fact true averages and true sums rather than nominal estimates, they constitute an *optimal* representation of the entire examination. Such an optimal representation enables a direct comparison (see Table F-1) of how dose values determined from a nominal analysis differ from those of a view-by-view analysis, since there is no confounding uncertainty in the magnitudes of the nominal values.

2. In a typical application of Method B, a user ordinarily will rely on estimated values of parameters for the entire examination that may be truly nominal. In this situation there are inaccuracies introduced to the extent that such nominal values differ from the optimal values. For example, if a user underestimates the total exposure with a nominal value of 100 R instead of 190 R in Table E-1, the user would obtain correspondingly underestimated nominal doses of 1.7 rad to the active bone marrow and 8.4 rad to the lungs.

Appendix F. Comparison of Results from Methods A and B

In Table F-1, the tissue doses estimated with Methods A and B are for the same sample examination given in Appendix D. Method A applies the view-by-view values and the approach indicated in Tables D-1 through D-4. Method B applies the approach indicated in Table E-1 to nominally represent the entire examination.

Table F-1. Adult Male LV/LCA/RCA — Tissue Doses for Entire Examination: Method A versus Method B

Tissue	Tissue Dose (rad) determined with Method A	Tissue Dose (rad) determined with Method B
Entrance skin in primary field (ESPF)	82 ^a	86 ^b
Brain	0.005	0.005
Thyroid	0.14	0.13
Thymus	1.8	1.8
Active bone marrow	3.7	3.3
Esophagus	11	9.2
Lung	17	16
Heart	20	18
Adrenal	13	18
Spleen	2.2	3.1
Pancreas	3.2	3.8
Stomach	1.5	1.8
Liver	3.2	2.7
Kidney	1.6	1.9
Colon	0.081	0.083
Small intestine	0.10	0.11
Urinary bladder	0.005	0.005
Testis	+	+

^aThe dose in the ESPF is the largest sum (in this case, 70 rad plus 11.9 rad, associated with Tables 9 and 3, respectively) of cumulative contributions to entrance skin sites sharing a common region of exposure. See page 23, footnote "g," and Appendix B, Figure B-2.

^bThe dose in the ESPF is the largest amount for any single skin location. It is the product of the interpolated conversion coefficient (950 mrad/R in this example) and the highest cumulative entrance exposure (90 R in this example) at any single skin location (estimated in this example from the sum 77 R plus 13 R, associated with Tables 9 and 3, respectively.)

+ Less than 0.001 rad.

APPENDIX G. Synopsis of Results for the Sample Examination

Absorbed Dose in the Entrance Skin in the Primary Field (Method A Results)

Because a variety of different views are used in the examination, no single area of entrance skin is uniquely irradiated throughout the examination. The largest single cumulative dose (82 rad) in a portion of ESPF occurs for the LAO 45° (Table 9) and LAO 30° (Table 3) views, where a common region of skin is irradiated (Figure B-2). Of all tissues, ESPF is at greatest risk for acute injury (i.e., erythema, epilation, or possibly more serious ulceration and necrosis). For this sample examination, depending on view, dose in the ESPF ranges from 3.7 to 82 rad, below the typical threshold of 200 rad (16) for early transient erythema.

Absorbed Dose in Internal Tissues (Method A Results)

Absorbed doses in internal tissues are cumulative for the entire examination. In this example, the total absorbed dose in lung tissue is 17.3 rad, and in active bone marrow (ABM) it is 3.7 rad. For the fields of view used, larger fractions of lung, esophageal, and adrenal tissues are in the radiation fields than other internal tissues at risk. Although the absorbed dose in the heart is larger, the heart is not subject to radiation risk at this level of dose. The magnitude of the absorbed dose in these tissues is relatively small compared to the maximum absorbed dose in the ESPF. The absorbed doses in the other internal tissues are an order of magnitude or more smaller than the absorbed doses in the lung, esophageal, and adrenal tissues.

Overall, the cineangiographic contribution to tissue doses is approximately one fifth of the fluoroscopic contribution. However, for any particular view, this ratio is not representative of the relative cineangiographic and fluoroscopic contributions to tissue dose. In approximately half of the views, the cineangiographic dose is about 3 times larger than the fluoroscopic dose. The overall result is skewed by the large fluoroscopic contribution (without any cineangiographic contribution) from the anterior view.

Comparison of Tissue Doses Estimated with Method A versus Method B

The largest percentage differences between tissue doses estimated with Method A versus Method B occur for the adrenal and spleen tissues, about $\pm 40\%$. The relative differences for other tissues are smaller. Because of the multiple views used in this sample examination, these differences are all significantly smaller than the maximum CV_{nom} values indicated in Table 12.